

Use of Electrochemical and SECM Techniques to Probe *Gingko biloba* Leaves Extract for Corrosion Inhibition of P110 Steel in 3.5% NaCl Solution Saturated with CO₂

Ambrish Singh^{1,2}, Yuanhua Lin^{1,*}, Eno. E. Ebenso^{4,5}, Wanying Liu¹, Bo Huang³,

¹State Key Laboratory of Oil and Gas Reservoir Geology and Exploitation (Southwest Petroleum University), Chengdu, Sichuan 610500, China.

² Department of Chemistry, LFTS, Lovely Professional University, Phagwara, Punjab 144402, India.

³ CNPC Key Lab for Tubular Goods Engineering (Southwest Petroleum University), Chengdu, Sichuan 610500, China.

⁴ Department of Chemistry, School of Mathematical & Physical Sciences, North-West University (Mafikeng Campus), Private Bag X2046, Mmabatho 2735, South Africa.

⁵ Material Science Innovation & Modelling (MaSIM) Focus Area, Faculty of Agriculture, Science and Technology, North-West University (Mafikeng Campus), Private Bag X2046, Mmabatho 2735, South Africa.

*E-mail: yhlin28@163.com; vishisingh4uall@gmail.com

Received: 4 April 2015 / Accepted: 7 July 2015 / Published: 28 July 2015

The effect of the leaves extract of *Gingko biloba* (GLE) as an inhibitor for P110 steel in 3.5% NaCl solution was studied using electrochemical and surface analysis techniques. The inhibition efficiency increased (95% EIS and 96% Tafel at 1000 ppm) with the increase in concentration of the inhibitor. Langmuir adsorption isotherm was followed by GLE showing a straight line with linear regression coefficient values. SEM and SECM analyses indicated that the corrosion mitigation was due to the adsorbed film of GLE on the metal surface.

Keywords: Steel; EIS; Polarization; Electrochemical calculation; SEM

1. INTRODUCTION

P110 casing steel can be used for H₂S situation of the northeast part of Sichuan Province and Tarim oil field, Xinjiang (China); furthermore, the reservoir usually contains CO₂, which makes the corrosion situation often more complex and worse. P110 can resist H₂S but does not resist CO₂ effectively in the reservoir. This motivated us to investigate the corrosion and inhibition of P110 steel in 3.5% NaCl solution.

Inhibitors are chemicals that are used to mitigate corrosion. The inhibitor mitigates corrosion by adsorbing on the metal surface and forming a thin layer [1-4]. Literatures reveal the use of several eco friendly corrosion inhibitors in different aggressive environments [5-13].

After the literature survey we concluded that no work has been reported on P110 steel in 3.5% NaCl solution saturated with CO₂. This motivated us to investigate the leaves extract of *Gingko biloba* (GLE) as potential corrosion inhibitor for the oil and gas pipeline steels.

2. EXPERIMENTAL

2.1. *Gingko leaves extract*

Dried *Gingko* leaves were ground to powder form. Dried (50 g) powder was soaked in ethanol (900 mL) and left for 24 hours. Next day, it was refluxed for 5 h and the extract was used to study the corrosion inhibition properties. P110 steel (wt.%): C 0.27; Si 0.26; Mn 0.6; P 0.009; S 0.003; Cr 0.5; Ni 0.25; Mo 0.6; Nb 0.05; V 0.005; Ti 0.02; Fe balance, was used for the electrochemical tests. P110 steel coupons having dimensions of 30 mm × 3 mm × 3 mm was used for the electrochemical study. CO₂ with 5 MPa pressure was pumped in the closed bottle containing 3.5% NaCl solution for 30 minutes.

2.2. *Electrochemical studies*

The impedance spectroscopy and Tafel polarization was performed through Autolab Potentiostat/Galvanostat (Model GSTAT302N) with FRC and GPES softwares for data fitting, and polarization curves. The four neck cells were used for electrochemical studies consisting of the working electrode, auxiliary electrode, reference electrode, and the fourth one was used to saturate CO₂ in the solution after which it was sealed.

The Tafel polarization studies were performed from -300 mV to +300 mV at a scan rate of 1 mV s⁻¹. The impedance studies were carried out from 100 kHz to 0.00001 kHz frequency range [14]. The corrosion inhibition efficiency ($\eta\%$) was evaluated using the following equation:

$$\eta\% = \frac{I_{\text{corr}}^0 - I'_{\text{corr}}}{I_{\text{corr}}^0} \times 100 \quad (1)$$

where, I_{corr}^0 and I'_{corr} are the corrosion current without inhibitor and in the presence of inhibitor, respectively. The inhibition efficiency of the inhibitor for Nyquist plot was calculated using the following equation:

$$\eta\% = \frac{R'_{\text{ct}} - R_{\text{ct}}^0}{R'_{\text{ct}}} \times 100 \quad (2)$$

where, R'_{ct} and R_{ct}^0 are the charge transfer resistance in presence of inhibitor and without inhibitor, respectively.

2.3. Scanning Electrochemical Microscopy (SECM)

The CHI900C was used with a 10 μm platinum tip of the probe for the scanning electrochemical microscopy studies. The cell assembly setup used was the same as used for the electrochemical test. The diameter of the samples was between 30 × 3 × 3 mm. The results were obtained at the tip at ~ 10 μm from the specimen surfaces at a scan rate of 80 μm/step [15, 16].

2.4. Scanning Electron Microscopy (SEM) and Energy-dispersive X-ray spectroscopy (EDX)

Micrographs of P110 steel surfaces with and without inhibitor were recorded using TESCAN VEGA II XMH device. EDX detector coupled with SEM device was used to analyze the changes in the composition of metal surface. All the specimens were dried before exposing the surface for imaging.

3. RESULTS AND DISCUSSION

3.1. EIS Measurement

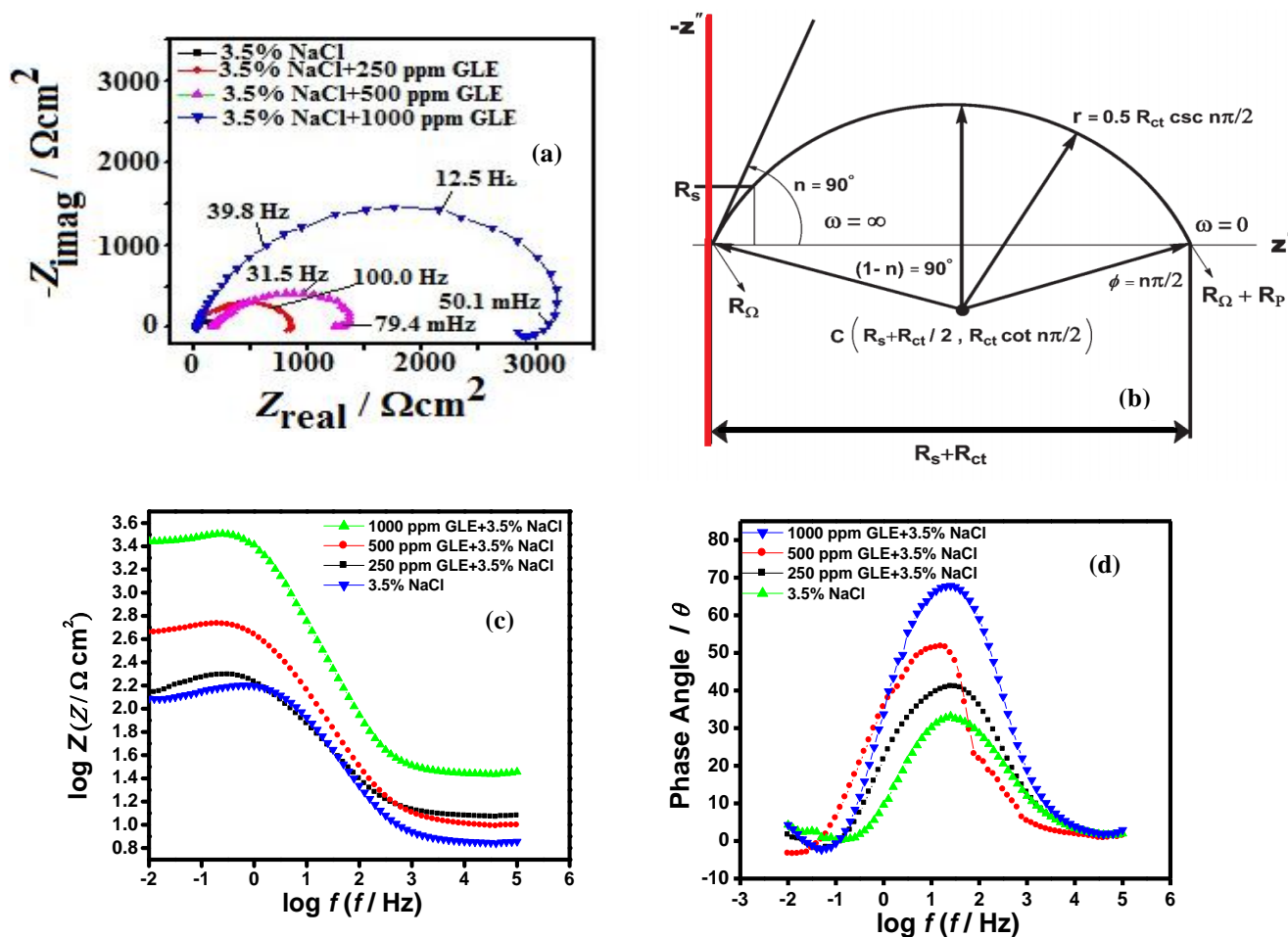


Figure 1. (a) Nyquist plots (b) Schematic diagram for Nyquist (c) Bode and (d) Theta- frequency plots for P110 steel in 3.5% NaCl solution in the absence and presence of GLE.

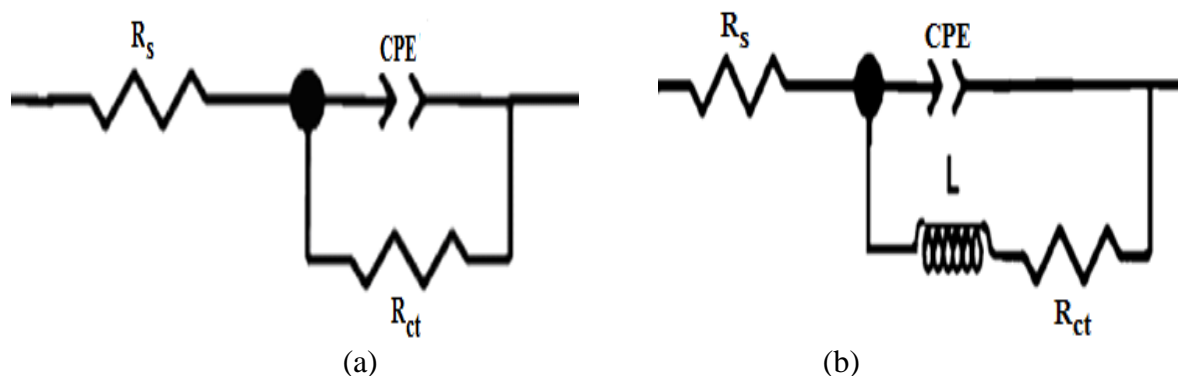


Figure 2. Model used for (a) 3.5% NaCl solution and (b) for GLE.

Fig. 1a shows the Electrochemical Impedance spectra for P110 steel as Nyquist plots at open circuit potential for P110 steel. Schematic Nyquist plots are represented in Fig. 1b. Bode plots (Fig. 1c) and the Theta frequency plots (Fig. 1d) were also studied and are shown respectively. The inhibition efficiency increases with the increase in inhibitor concentration. This is evidenced by the diameter of the Nyquist plots that gets bigger with each increasing concentration. The impedance spectra for 3.5% NaCl solution was analyzed by using the equivalent circuit (Fig. 2a) while of GLE was analyzed by another equivalent circuit having inductance in addition to R_s , R_{ct} and CPE (Fig. 2b). CPE is derived from equations (3) and (4) [17-20]:

$$Z_{CPE} = R_s + \frac{R_{ct}}{1 + R_{ct}Y(j\omega)^n} \tag{3}$$

$$\left(j\omega \right)^n = \omega^n e^{j\frac{n\pi}{2}} = \omega^n \left(\cos \frac{n\pi}{2} + j \sin \frac{n\pi}{2} \right) \tag{4}$$

By inserting equation (3) into equation (4) and, if $Z_{CPE} = Z + jZ'$, we get the following relation:

$$\left(Z' - R_s - \frac{R_{ct}}{2} \right)^2 + \left(-Z^n + R_{ct} \cot \frac{n\pi}{2} \right)^2 = \left(\frac{R_{ct}}{2} \csc \frac{n\pi}{2} \right)^2 \tag{5}$$

C_{dl} can be obtained at center $C (R_s + R_{ct}/2, R_{ct} \cot n\pi/2)$, the maximum in Nyquist plot when $Z = (R_s + R_{ct})/2$, this happens when $1 - R_{ct}^2 (Y\omega_{max}^n)^2 = 0$, this solution implies that $R_{ct} Y\omega^n = 1$, and thus:

$$\omega^n = \frac{1}{R_{ct}Y} \tag{6}$$

The double-layer capacitance (C_{dl}) values can be calculated from CPE values using the following equation as shown in table 1 [21-24]:

$$C_{dl} = \left(\frac{Y\omega^{n-1}}{\sin(n(\pi/2))} \right) \tag{7}$$

where, ω is the angular frequency, i.e., $2\pi f_{max}$. The (τ) can be calculated according to the equation:

$$\tau = \frac{1}{2\pi f_{\max}} \tag{8}$$

The relaxation time of a surface state is defined by the following equation:

$$\tau = C_{dl}R_{ct} \tag{9}$$

The values of τ with the chi-square value of the fitting are given in table 1 [25, 26]. The interface parameter (τ) decreased from 496.2 sec to 19.6 sec while the capacitance (C_{dl}) value decreased from 79.8 to 27.9 $\mu\text{F cm}^{-2}$ with the increase in the inhibitor concentration up to 1000 ppm [27-29].

The electrochemical impedance parameters such as inhibition efficiency ($\eta\%$), solution resistance (R_s), charge transfer resistance (R_{ct}), phase shift (n), and inductance (L) are listed in table 1. Nyquist plots showed that the diameter of P110 steel with inhibitor changes significantly in comparison to the solution without inhibitor. From table 1, it is clear that the greatest effect was observed at 1000 ppm of GLE that gives R_{ct} value of 3157 $\Omega \text{ cm}^2$ in 3.5% NaCl respectively.

Table 1. Electrochemical impedance parameters for P110 steel in the absence and presence of GLE.

Sol	R_s	R_{ct}	n	Y_0	τ	C_{dl}	L	Chi	η	Surf. Coverage
	($\Omega \text{ cm}^2$)	($\Omega \text{ cm}^2$)		($\Omega^{-1} \text{ s}^n / \text{cm}^2$)	(sec)	($\mu\text{F cm}^2$)	(H cm^2)	Square	%	θ
3.5% NaCl	2.5	145	0.848	246	496.2	79.8	-	0.0006	-	-
GLE 250 ppm	3.2	850	0.837	113	157.0	40.8	81	0.0008	83	0.83
GLE 500 ppm	1.7	1294	0.852	77	49.4	36.1	104	0.0033	89	0.89
GLE 1000 ppm	1.2	3014	0.871	48	19.6	27.9	93	0.0019	95	0.95

The values of $\log|Z|$ vs. $\log f$ (0.470–0.719) were close to -1 and the phase angle values for blank 3.5% NaCl (-33.4°), GLE 250 ppm (-41.3°), GLE 500 ppm (-51.1°) and GLE 1000 ppm (-69.7°) can be observed (table 2). A slope of -1 and a phase angle of -90° represents an ideal capacitive behavior [30-32].

Table 2. The slope of Bode plots and phase angles (α) for P110 steel in absence and presence of GLE.

C (ppm)	-S	- α°
3.5% NaCl	0.470	33.4
GLE 250 ppm	0.482	41.3
GLE 500 ppm	0.641	51.1
GLE 1000 ppm	0.719	69.7

3.2. Polarization Measurements

Fig. 3 shows the polarization curves for P110 steel in presence and absence of GLE in 3.5% NaCl solution. Table 3 gives the values of corrosion current (I_{corr}), corrosion potential (E_{corr}), cathodic and anodic Tafel slopes (b_c , b_a) and inhibition efficiency ($\eta\%$). According to the literatures, [33, 34] (i) if displacement in corrosion potential is <85 , the inhibitor can be mixed type. In the present study, shift in E_{corr} values is in the range of 32 mV, suggesting that GLE act as mixed type of inhibitor [35, 36].

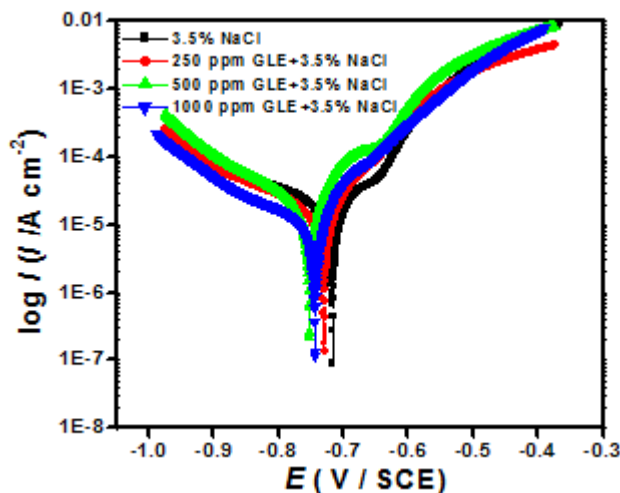


Figure 3. Tafel Polarization curves for P110 steel with and without GLE.

Table 3. Tafel Polarization parameters for P110 steel with and without GLE.

Conc.(ppm)	E_{corr}	I_{corr}	b_a	$-b_c$	η	Surface coverage
	(V vs. SCE)	(A cm ⁻²)	(V d ⁻¹)	(V d ⁻¹)	(%)	θ
3.5% NaCl	-0.721	9.1	0.06	1.03	-	-
GLE 250 ppm	-0.732	1.9	0.08	0.81	79	0.79
GLE 500 ppm	-0.753	1.3	0.04	0.56	86	0.86
GLE 1000 ppm	-0.750	0.4	0.06	0.27	96	0.96

3.3. Adsorption characteristics of the inhibitor

The adsorption of GLE molecules on the metal surface can be considered as a process between the inhibitor ($Inh_{(sol)}$) and water molecules ($H_2O_{(ads)}$) [37].



where, x is the size ratio representing the number of water molecules replaced by one molecule of the organic inhibitors. Langmuir adsorption isotherm was used according to the equation given below:

$$\theta = \frac{K_{ads}C_{inh}}{1+K_{ads}C_{inh}} \tag{Langmuir isotherm} \tag{11}$$

This equation can be rearranged to

$$\frac{C_{inh}}{\theta} = \frac{1}{K_{ads}} + C_{inh} \tag{12}$$

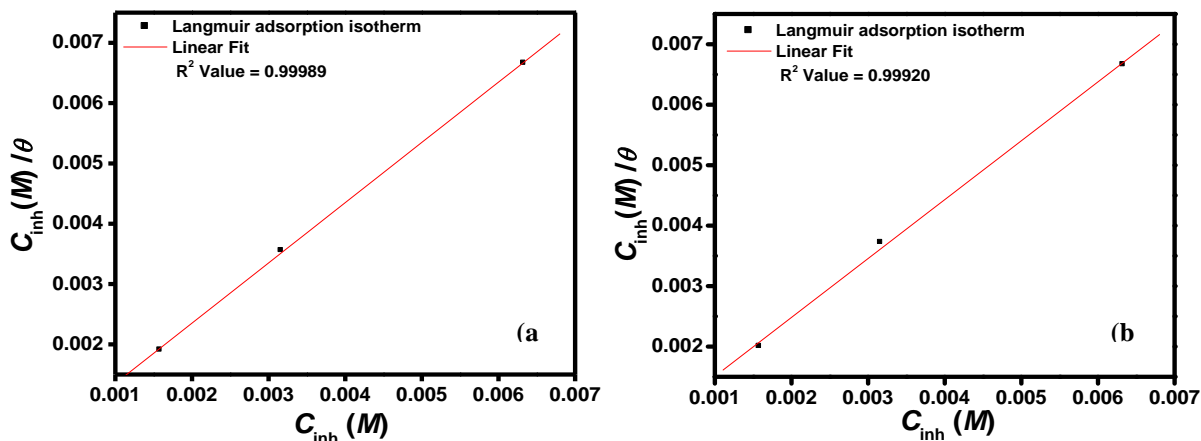


Figure 4. Langmuir adsorption isotherm plots for (a) EIS and (b) Tafel.

Fig. 4a, 4b represents a straight-line graph of C_{inh} versus values of C_{inh}/θ . The correlation coefficients were almost linear (R^2) ranging 0.99989 for EIS and 0.99920 for Tafel polarization obtained from plots of the GLE which indicated the adsorption of GLE on the P110 steel surface obeyed Langmuir adsorption isotherm [38, 39]. K_{ads} can be related to free energy of adsorption, ΔG_{ads} as [40]:

$$\Delta G_{ads}^{\circ} = -RT \ln(55.5 K_{ads}) \tag{13}$$

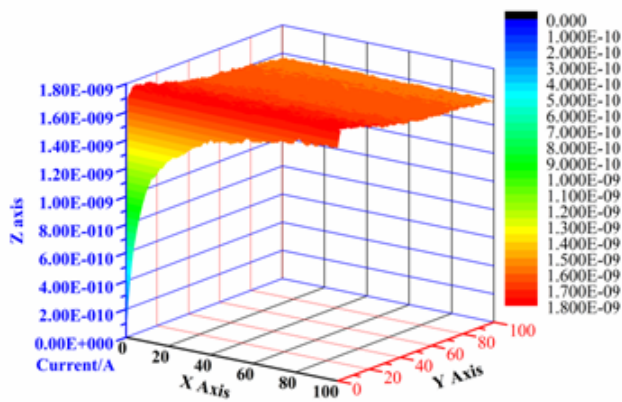
The values of K_{ads} and ΔG_{ads}° are given in table 4. The spontaneity of the adsorption process was confirmed by the negative values of ΔG_{ads}° [41, 42].

Table 4. Thermodynamic parameters for the adsorption of GLE on the P110 steel at different concentrations.

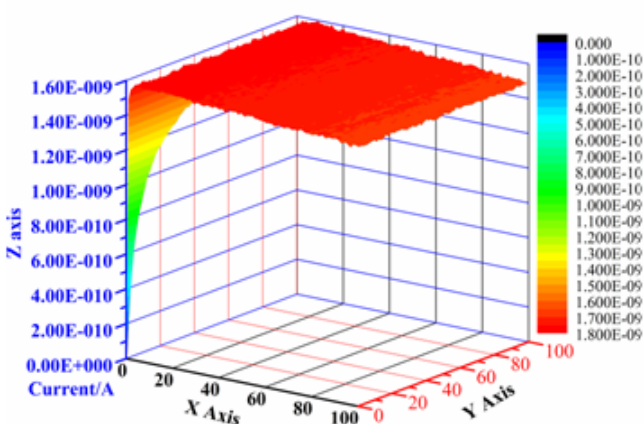
	EIS		Tafel	
Concentration	K_{ads}	ΔG_{ads}°	K_{ads}	ΔG_{ads}°
M	M^{-1}	$kJ\ mol^{-1}$	M^{-1}	$kJ\ mol^{-1}$
3.5% NaCl	-	-	-	-
1000 ppm GLE	3967	-30.4	5011	-31.0

3.4. Scanning Electrochemical Microscopy (SECM)

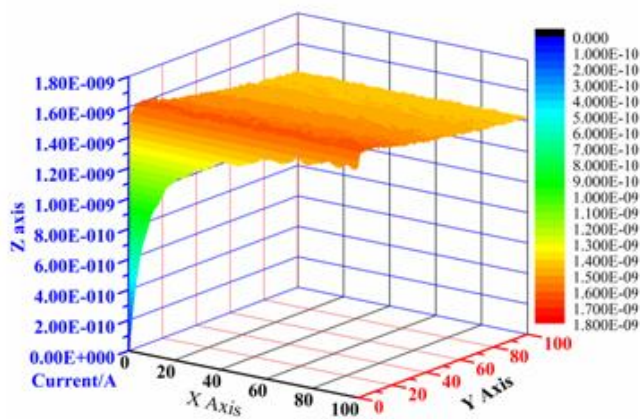
Fig. 5a-h shows the images of the samples as observed under scanning electrochemical microscope. The distance between the probe and the sample was established by approach curves prior to each experiment.



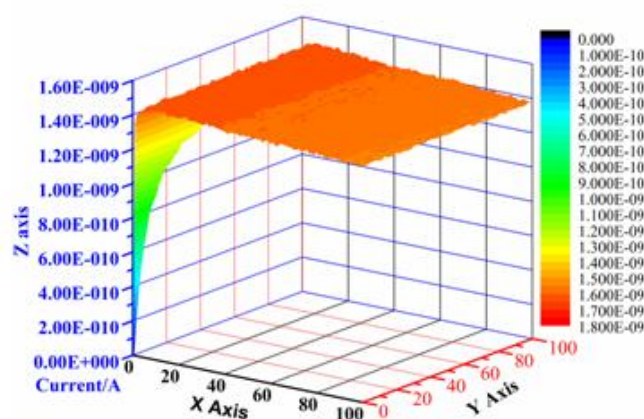
(a)



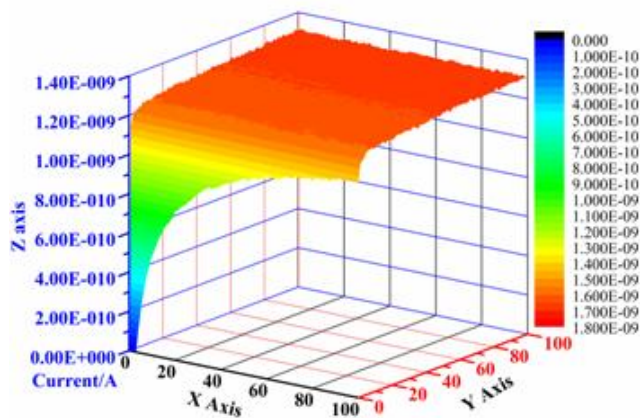
(b)



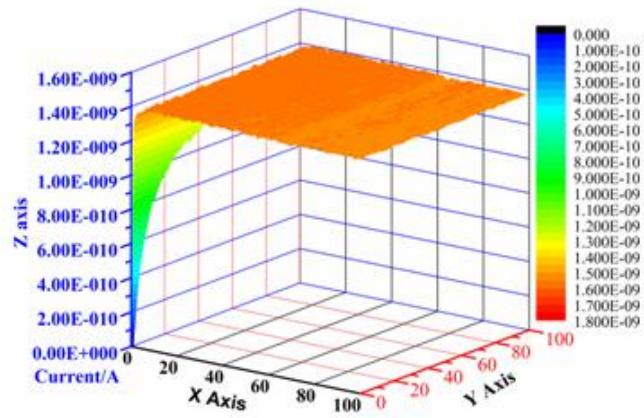
(c)



(d)



(e)



(f)

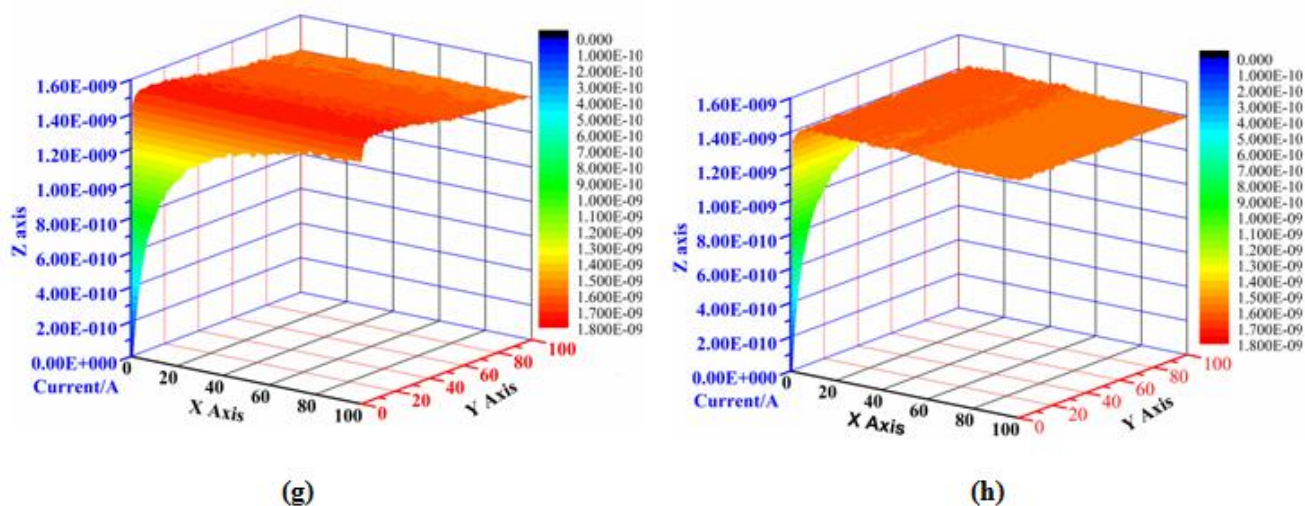


Figure 5. SECM figures for (a) 3.5% NaCl *x* axis (b) 3.5% NaCl *y* axis (c) 250 ppm GLE *x* axis (d) 250 ppm GLE *y* axis (e) 500 ppm GLE *x* axis (f) 500 ppm GLE *y* axis (g) 1000 ppm GLE *x* axis and (h) 1000 ppm GLE *y* axis.

When an insulating surface (GLE inhibitor) covering the steel surface is approached by the probe, there is hindrance in the diffusion current and the tip current decreases (Fig. 5c-h). The current increases when a conducting, *i.e.* blank 3.5% NaCl solution without GLE inhibitor is approached (Fig. 5a, b) [43-48].

3.5. Scanning Electron Microscopy (SEM) and EDX

The P110 steel surface was analyzed using scanning electron microscopy to show the corrosion mitigation by GLE. The specimen surface in Fig. 6a showed a strongly damaged and corroded surface without inhibitors. Fig. 6b showed a less damaged surface in 3.5% NaCl solution with 250 ppm GLE. The surface was smooth for 500 ppm and 1000 ppm of GLE as shown in Fig. 6c and Fig. 6d. These results indicated that the GLE blocked the active centers on the metal surface thereby effectively mitigating corrosion.

The elements present on the P110 steel surface were analyzed through an EDX spectrum. Fig. 7a is the EDX spectrum of the P110 steel without GLE that indicates the presence of Fe, Mn, Zn, Cr, Mg, Si, As peaks, which led to the breakdown at the metal surface and easy corrosion of bare metal. Spectra of Fig. 7b, 7c and 7d showed that the metal peaks are significantly suppressed compared to the P110 steel surface in presence of GLE. The peaks were suppressed due to the GLE molecules on the P110 steel that covered the active centers and hence the corrosion was mitigated.

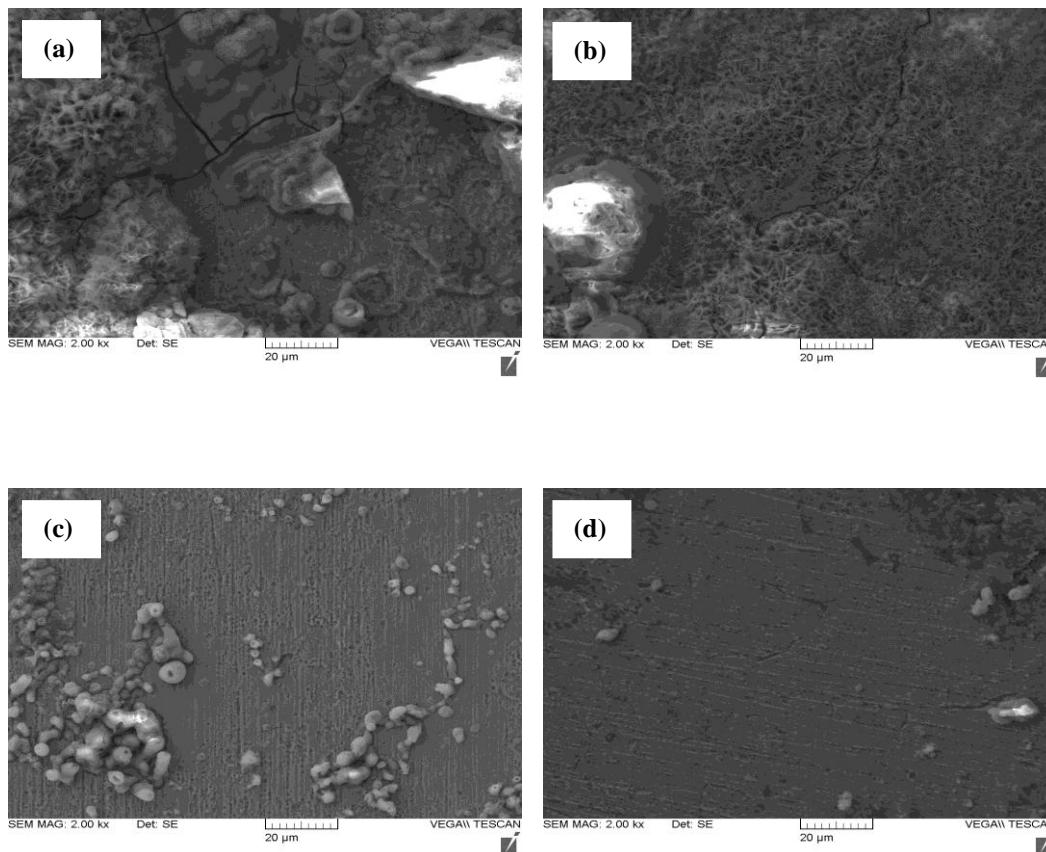
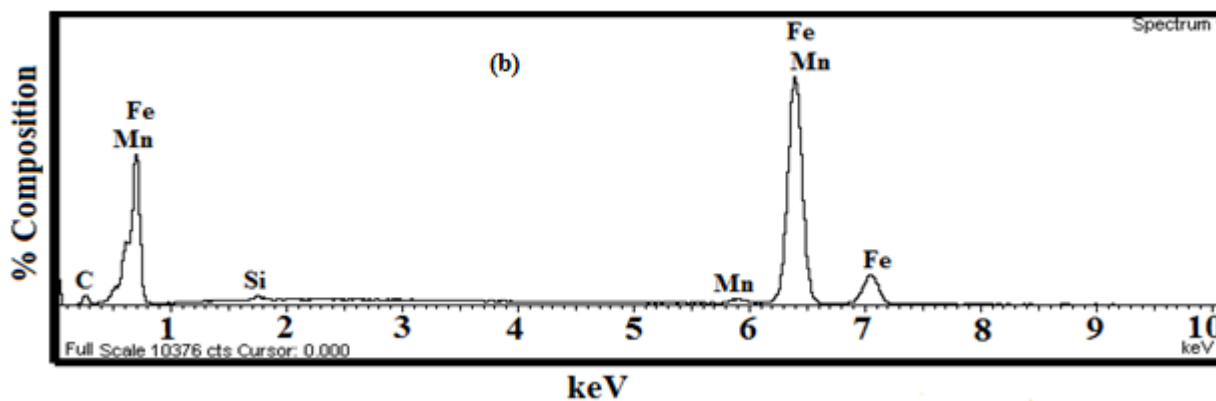
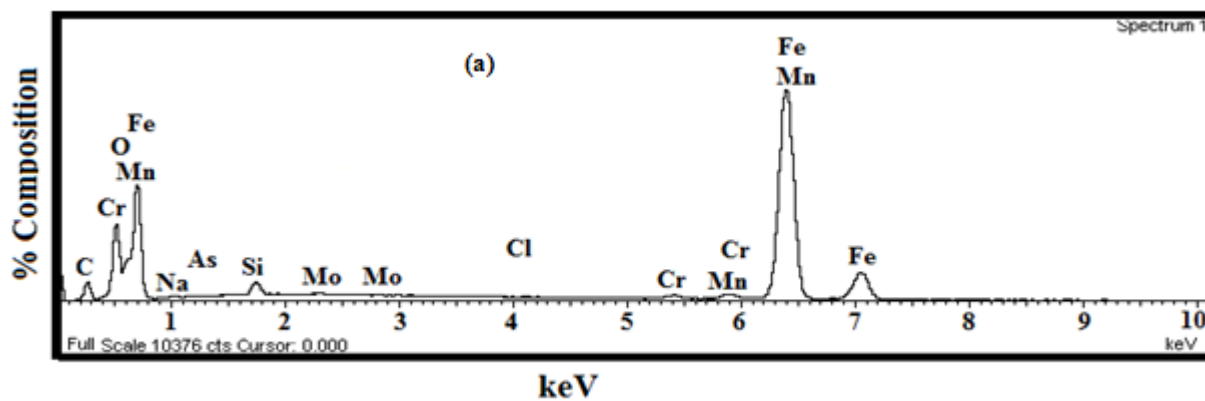


Figure 6. SEM images for (a) 3.5% NaCl solution (b) 250 ppm GLE (c) 500 ppm GLE and (d) 1000 ppm GLE.



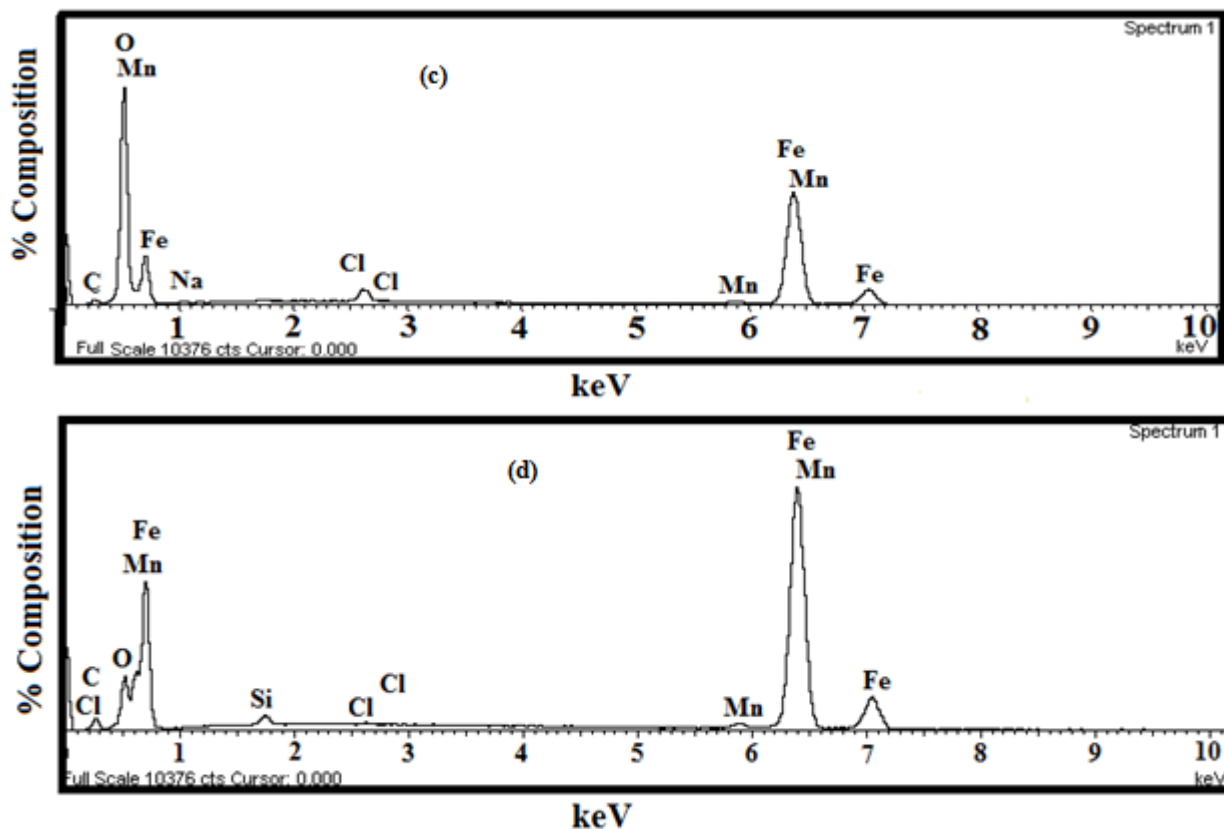


Figure 7. EDX peaks for (a) 3.5% NaCl solution (b) 250 ppm GLE (c) 500 ppm GLE and (d) 1000 ppm GLE.

5. CONCLUSIONS

1. The inhibition efficiency increases with the increase in concentration of GLE effectively.
2. Langmuir adsorption isotherm was followed by the adsorption of GLE molecules on the P110 steel surface.
3. Tafel Polarization values indicated that GLE acted as mixed type inhibitor.
4. The SECM and SEM-EDX analyses showed that GLE can effectively mitigate the corrosion of P110 steel.

ACKNOWLEDGEMENTS

Authors are thankful for the project fund from National Natural Science Foundation of China (No. 51274170), Sichuan Province project and Open Fund (PLN1411) of State Key Laboratory of Oil and Gas Reservoir Geology and Exploitation, Southwest Petroleum University.

References

1. K. R. Ansari, M. A. Quraishi, A. Singh, *Corros. Sci* 79 (2014) 5

2. A. Singh, Y. Lin, W. Liu, D. Kuanhai, J. Pan, B. Huang, C. Ren, D. Zeng, *J. Tai. Inst. Chem. Eng.* 45 (2014) 1918
3. H. M. Abd El-Lateef, L. I. Aliyeva, V. M. Abbasov, T. I. Ismayilov, *Adv. Appl. Sci. Res.* 3 (2012) 1185
4. A. Singh, Y. Lin, E. E. Ebenso, W. Liu, J. Pan, B. Huang, *J. Ind. Eng. Chem.* (2014) [http://doi: 10.1016/j.jiec.2014.09.034](http://doi.org/10.1016/j.jiec.2014.09.034)
5. A. Singh, V. K. Singh, M. A. Quraishi, *Arab J Sci Engg.* 38 (2013) 85
6. I. Ahamad, R. Prasad, M. A. Quraishi, *Corros. Sci.* 52 (2010) 933
7. A. Singh, M. A. Quraishi, *Res. Chem. Intermed.* 41 (2015) 2901
8. M. A. Quraishi, A. Singh, V. K. Singh, D. K. Yadav, A. K. Singh, *Mater. Chem. Phys.* 122 (2010) 114
9. G. Husnu, S. H. Ibrahim, *Ind. Eng. Chem. Res.* 51 (2012) 785
10. A. Singh, I. Ahamad, V. K. Singh, M. A. Quraishi, *Chem. Eng. Comm.* 199 (2012) 63
11. A. Teris, B. Van, *J. Chromatog. A* 967 (2002) 21
12. G. Chen, M. Zhang, J. Zhao, R. Zhou, Z. Meng, J. Zhang, *Chem. Cent. J.* 7 (2013) 83
13. A. A. Al-Amiery, Y. K. Al-Majedy, A. A. H. Kadhum, A. B. Mohamad, *Molecules* 20 (2015) 366
14. B. Evgenij, J. R. Macdonald, *Impedance Spectroscopy Theory, Experiment, and Applications*, John Wiley & Sons, New Jersey, (2005).
15. A. J. Bard, F. R. F. Fan, J. Kwak, O. Lev, *Anal. Chem.* 61 (1989) 132
16. C. Lee, A. J. Bard, *Anal. Chem.* 62 (1990) 1906
17. A. Singh, I. Ahamad, V. K. Singh, M. A. Quraishi, *J. Solid State Electrochem.* 15 (2011) 1087
18. A. O. Yuce, R. Solmaz, G. Kardas, *Mater. Chem. Phys.* 131 (2012) 615
19. J. B. Perez-Navarrete, C. O. Olivares-Xometl, N. V. Likhanova, *J. Appl. Electrochem.* 40 (2010) 1605
20. D. K. Yadav, D. S. Chauhan, I. Ahamad, M. A. Quraishi, *RSC. Adv.* 3 (2013) 632
21. R. A. Bustamante, G. N. Silve, M. A. Quijano, H. H. Hernandez, M. R. Romo, A. Cuan, M. P. Pardave, *Electrochim. Acta* 54 (2009) 5393
22. C. Montecelli, F. Zucchi, G. Brunoro, G. Trabaneli, *J. Appl. Electrochem.* 27 (1997) 325
23. H. Gerengi, H.I. Sahin, *Ind. Eng. Chem. Res.* 51 (2012) 780
24. M.A. Amin, K.F. Khaled, *Corros. Sci.* 52 (2010) 1762
25. K. R. Ansari, Sudheer, Ambrish Singh, M. A. Quraishi, *J. Disp. Sci. Tech.* (2014) [http://doi: 10.1080/01932691.2014.938349](http://doi.org/10.1080/01932691.2014.938349)
26. Y. Lin, A. Singh, Y. Wu, C. Zhu, H. Zhu, E. E. Ebenso, *J. Tai. Inst. Chem. Eng.* (2014) [http://doi: 10.1016/j.jtice.2014.09.023](http://doi.org/10.1016/j.jtice.2014.09.023).
27. D. K. Yadav, M. A. Quraishi, *Ind. Eng. Chem. Res.* 51 (2012) 14966
28. K.R. Ansari, M.A. Quraishi, A. Singh, *J. Ind. Eng. Chem.* (2014) <http://dx.doi.org/10.1016/j.jiec.2014.10.017>.
29. M. Lebrini, M. Lagrene'e, H. Vezin, M. Traisnel, F. Bentiss, *Corros. Sci.* 49 (2007) 2254
30. K. F. Khaled, M. A. Amin, *Corros. Sci.* 51 (2009) 1964
31. D. K. Yadav, M. A. Quraishi, B. Maiti, *Corros. Sci.* 55 (2012) 254
32. M. Lebrini, F. Robert, A. Lecante, C. Roos, *Corros. Sci.* 53 (2011) 687.
33. H. H. Hassan, *Electrochim. Acta* 53 (2007) 1722
34. Lorenz, W.J., Mansfeld, F., *Corros. Sci.* 21(1981) 647.
35. A. Singh, Y. Lin, C. Zhu, Y. Wu, E. E. Ebenso, *Chin. J. Poly. Sci.* 33 (2014) 339
36. M.S. Morad, *Mater. Chem. Phys.* 60 (1999) 188.
37. 44:467–479G. Ji, P. Dwivedi, S. Sundaram, R. Prakash, *Ind. Eng. Chem. Res.* 52 (2013) 10673
38. S. Andreani, M. Znini, L. M. Paolini, B. Hammouti, J. Costa, A. Muselli, *Int. J. Electrochem. Sci.* 8 (2013) 11896
39. K. M. Ismail, *Electrochim. Acta* 53 (2008) 5953

40. C.B. Verma, M.A. Quraishi, A. Singh, *J. Taiwan Inst. Chem. Eng.* (2014)
<http://doi:10.1016/j.jtice.2014.11.029>.
41. M. Yadav, D. Behera, U. Sharma, *Arab. J. Chem.* DOI: 10.1016/j.arabjc.2012.03.011
42. H. Keles, M. Keles, I. Dehri, O. Serindag, *Colloid Surface A* 320 (2008) 138
43. E. E. Oguzie, B. N. Okolue, E. E. Ebenso, G. N. Onuoha and A. I. Onuchukwu, *Mater Chem Phy.*, 87(2-3), (2004) 394-401.
44. K.R. Ansari, M.A. Quraishi, A. Singh, *Corros. Sci.* (2015)
<http://dx.doi.org/10.1016/j.corsci.2015.02.010>.
45. B. M. Quinn, I. Prieto, S. K. Haram, A. J. Bard, *J. Phys. Chem. B* 105 (2001) 7474
46. M. Tsionsky, A. J. Bard, D. Dini, F. Decker, *Chem. Mater.* 10 (1998) 2120
47. A. Maljusch, C. Senoz, M. Rohwerder, W. Schuhmann, *Electrochim. Acta* 82 (2012) 339
48. J. Izquierdo, L. Nagy, J. J. Santana, G. Nagy, R. M. Souto, *Electrochim. Acta* 58 (2011) 707
49. C.B. Verma, M.A. Quraishi, Ambrish Singh, *J. Tai. Inst. Chem. Eng.* (2014)
<http://doi:10.1016/j.jtice.2014.11.029>
50. A. Singh, Y. Lin, W. Liu, S. Yu, J. Pan, C. Ren, D. Kuanhai, *J. Ind. Eng. Chem.* (2014) <http://doi:10.1016/j.jiec.2014.01.033>
51. A. Singh, I. Ahamad, M. A. Quraishi, *Arab. J. Chem.* (2012)
<http://dx.doi.org/10.1016/j.arabjc.2012.04.029>
52. C. Kamal, M. G. Sethuraman, *Ind. Eng. Chem. Res.* 51 (2012) 10399-10407.

© 2015 The Authors. Published by ESG (www.electrochemsci.org). This article is an open access article distributed under the terms and conditions of the Creative Commons Attribution license (<http://creativecommons.org/licenses/by/4.0/>).